A Novel Form of Pigment-Dispersing Hormone in the Central Nervous System of the Intertidal Marine Isopod, *Eurydice pulchra* (Leach)

David C. Wilcockson,[1] Lin Zhang,[2] Michael H. Hastings,[3] Charalambos P. Kyriacou,[2] and Simon G. Webster[4]*

[1]Institute of Biological Environmental and Rural Sciences, Aberystwyth University, Penglais, Aberystwyth, Ceredigion, SY23 3DA, United Kingdom
[2]Department of Genetics, University of Leicester, Leicester, LE1 7RH, United Kingdom
[3]MRC Laboratory of Molecular Biology, Cambridge, CB2 0QH, United Kingdom
[4]School of Biological Sciences, Bangor University, Bangor, Gwynedd, LL57 2UW, United Kingdom

ABSTRACT

Pigment-dispersing factor (PDF) is well known as a circadian clock output factor, which drives daily activity rhythms in many insects. The role of its homologue, pigment-dispersing hormone (PDH), in the regulation of circadian and/or circatidal rhythmicity in crustaceans is, however, poorly understood. The intertidal isopod crustacean, *Eurydice pulchra* has well-defined circatidal (12.4-hour) activity rhythms. In this study we show that this runs parallel to a circadian (24-hour) cycle of chromatophore dispersion. As a first step in determining the potential role of PDH in these rhythms, we have identified a novel form of PDH expressed in this species. Because conventional homology cloning was unsuccessful, we employed immuno-identification and Edman microsequencing to determine the primary structure of this peptide. From this, cDNA cloning identified the nucleotide encoding sequence and thus facilitated description of PDH neurons by in situ hybridization and immunohistochemistry. We show them to be morphologically similar to those that co-ordinate circadian activity rhythms in insects. In animals expressing both tidal (activity) and circadian (chromatophore) rhythms, however, there was no evidence for a corresponding periodicity in the expression of *pdh* transcript, as determined by quantitative reverse transcriptase polymerase chain reaction (qRT-PCR) in *Eurydice* heads. It is therefore suggested that any role for PDH in daily/tidal timing in *Eurydice* is not mediated at the transcriptional level, rather rhythms in neurohemal release may be important in such co-ordination. J. Comp. Neurol. 519: 562–575, 2011.

INDEXING TERMS: Indexing terms: pigment-dispersing hormone; circadian rhythms; isopod; *Eurydice pulchra*; gene expression; in situ hybridization; immunohistochemistry; quantitative RT-PCR

The pigment-dispersing hormones (PDHs) of crustaceans form a large group of structurally related octadecapeptides, whose established functions involve dispersion of mainly black pigment granules in the chromatophores and light adaptational movements of screening pigments in the ommatidia (for reviews, see Rao and Riehm, 1989, 1993; Rao, 2001). Structurally related hormones—pigment-dispersing factors (PDFs)—are ubiquitous in insects, in which they are important in modulation of circadian rhythms. PDF immunoreactivity is found in circadian pacemaker neurons that express *period* and *timeless* near the accessory medulla of *Drosophila* brains (Helfrich-Förster, 1995), and misexpression of PDF severely disrupts rhythmic behavior in flies (Renn et al., 1999; Helfrich-Förster et al., 2000). Knockdown of PDF by RNAi abolishes circadian rhythmicity in *Blatella* (Lee et al., 2009), and injected peptide shifts the phase of the circadian pacemaker in the cockroach *Leucophaea* (Petri and Stengl, 1997). PDF is also involved in circadian

Grant sponsor: The Biotechnology and Biological Sciences Research Council (BBSRC); Grant numbers: 91/S17172, BBE0017501 and BB/E000835/1; Grant sponsors: The Royal Society; Wolfson Research Merit Award (to C.P.K).

*CORRESPONDENCE TO: S. G. Webster, School of Biological Sciences, Bangor University, Bangor, Gwynedd, LL57 2UW, UK.
E-mail: s.g.webster@bangor.ac.uk

Received July 11, 2010; Revised August 27, 2010; Accepted September 28, 2010
DOI 10.1002/cne.22533
Published online October 28, 2010 in Wiley Online Library (wileyonlinelibrary.com)

morphological changes in the eyes of *Musca domestica* (Pyza and Meinertzhagen 1996, 1997, 1998; Pyza, 2002), and some neurites of PDF-expressing neurons exhibit circadian changes in morphology (Pyza and Meinertzhagen, 1997; Miśkiewicz et al., 2008).

The neuroanatomy of PDH-expressing cells has been described in a variety of decapod crustaceans (Dircksen et al., 1987, Mangerich et al., 1987; Mangerich and Keller, 1988; Hsu et al., 2008), an isopod (Nussbaum and Dircksen, 1995), barnacles (Webster, 1998), and a copepod (Sousa et al., 2008). For insects, many reports have detailed PDH-immunoreactive neurons in several orders (i.e., Homberg et al., 1991; Sehadová et al., 2003; for review, see Homberg, 1994). The apparent ubiquity of PDH/PDF peptides in arthropods, and its role as a key output gene in insect circadian biology, suggest that it may play a similar role in crustacean circadian biology. This view is supported by morphological comparisons between the optic lobes of crustaceans and insects (Strausfeld, 2005) and PDH-immunoreactive neurons (Harzsch et al., 2009). Indeed, many crustaceans show discrete circadian rhythmicity patterns, for example, in locomotor activity (for reviews, see Naylor, 1996, 2010; Palmer, 2001) and retinal sensitivity (Aréchiga and Rodriguez-Sosa, 1998; Fanjul-Moles and Prieta-Sagredo, 2003). The circadian changes in the electroretinogram of crayfish can be phase-shifted by bath application of PDH (Verde et al., 2007). Circadian rhythmicity in chromatophore dispersion in a variety of crustaceans has also been well documented (Abramowitz, 1937; Brown et al., 1953; Powell, 1962). This 24-hour cycle is superimposed in neritic or intertidal crustaceans upon distinct circatidal (or circalunidian) rhythms, with a period (tau) of approximately 12.4 hours.

Putative candidate clock components in crustaceans (neuropeptides as well as canonical clock genes) have recently been comprehensively reviewed (Strauss and Dircksen, 2010). Important questions remain, particularly on the role of PDH in crustacean rhythmicity and the clockwork. Might this peptide also be involved in maintenance of circatidal rhythmicity? To begin to answer these questions, we have used the intertidal marine isopod *Eurydice pulchra*, which displays robust circatidal rhythmicity, modulated by a strong circadian component (Hastings, 1981a,b). First we identified a novel PDH-like peptide from *Eurydice* brains/optic ganglia by classical Edman microsequencing and subsequent cloning and sequencing of its cognate mRNA in *Eurydice*. Second, we determined the neuroanatomy of PDH-expressing neurons in the brain and optic ganglia by immunohistochemistry (IHC) and in situ hybridization (ISH), which revealed complete co-localization of mRNA and peptide in all somata. The projection patterns of immunolabeled neurons and neurites are in accord with those found in the circadian pacemaker neurons of insects. Finally, expression patterns of PDH were examined by quantitative reverse transcriptase polymerase chain reaction (qRT-PCR), together with determination of endogenous rhythms of chromatophore dispersion and swimming behavior, in an attempt to correlate any changes in PDH gene expression with circadian and tidal phenotypes.

MATERIALS AND METHODS

Animals and tissue collection

Specimens of adult (3–6-mm) *Eurydice pulchra* were collected by a hand-pulled trawl from the surf zone of Llanddona Beach, Anglesey, UK, and maintained in darkness in 20-liter containers at 15°C. Animals were anesthetized on ice prior to decapitation. For peptide isolation, cloning, and qRT-PCR, heads were immediately placed in liquid nitrogen and stored at −80°C until use. For ISH, nervous systems were microscopically dissected in ice-cold physiological saline and fixed in 4% paraformaldehyde (PFA) in 50 mM phosphate-buffered saline (PBS) for 4 hours, at room temperature, followed by brief washing in PBS and dehydration in a graded methanol/PBS series. Tissues were subsequently stored in 100% methanol for up to 3 days at −20°C. For IHC, nervous systems were fixed (overnight, 4°C) in Stefanini's fixative (Stefanini et al., 1967) and washed extensively in PTX (PBS, 0.1% Triton X-100, 0.02% NaN_3).

Isolation of PDH

Heads from about 1,500 *Eurydice* were homogenized (in batches of approximately 250) in 200 μl ice-cold 2 M acetic acid, centrifuged (30,000*g*, 15 minutes, 4°C) and immediately dried in a vacuum centrifuge. These extracts were dissolved in water, re-centrifuged, and applied (in batches of approximately 750 head equivalents) to solid-phase extraction columns (Strata-X 33 μm polymeric reversed phase 200 mg, Phenomenex, Macclesfield, UK) previously conditioned with isopropanol. After washing unbound material (in 10 ml of water), peptides were eluted with 3 ml 60% isopropanol and immediately dried. Peptides were separated in batches of 200–250 head equivalents by high-performance liquid chromatography (HPLC; Dionex Summit, Dionex, Sunnyvale, CA). Conditions were as follows: column, Jupiter (Phenomenex) 250 × 4.6 mm, 300 Å C_{18}; solvents, A, 0.11% trifluoroacetic acid (TFA) and B, 60% acetonitrile containing 0.1% TFA; gradient: 40–80% B over 40 minutes, 1 ml/min, with detection at 210 nm. Then 0.5-ml fractions were collected and immediately dried. Screening of fractions for PDH was performed by enzyme immunoassay (EIA).

Dried fractions (10 head equivalents) were dissolved in 0.1 M bicarbonate buffer, pH 9.3, and coated (100 μl,

overnight, 4°C) onto 96-well plates (Corning 3590, Corning, NY). Plates were washed in the same buffer and blocked (0.1% bovine serum albumin [BSA]), prior to incubation in anti-PDH (1:1,000, 4°C, overnight). After extensive washing in PBST (50 mM PBS, 0.1% Tween 20) and incubation in 1:5,000 peroxidase-labeled goat-anti rabbit IgG (Vector, Burlingame, CA), immunoreactive (IR) fractions were visualized with ABTS solution (0.04% 2, 2′-azino-bis [3-ethylbenzothiazoline-6 sulphonic acid] diammonium salt, 0.02% hydrogen peroxide [30%] in 0.1 M phosphate citrate buffer, pH 4.0). Immunopositive fractions were rechromatographed by using a shallower gradient (40–80% B over 1 hour) and rescreened for PDH immunoreactivity. Material representing 90% of the peptide isolated (approximately 30 pmol) was subjected to automated Edman microsequencing (Cambridge Peptides, Birmingham, UK). For mass determination, approximately 3 pmol of PDH-IR material was dissolved in 2 μl acetonitrile and mixed with an equal volume of 10% α-cyano-4 hydroxycinnamic acid (CHCA) in 30% acetonitrile, 0.1% TFA; 1 μl was spotted on a stainless steel target. Matrix-assisted laser desorption/ionization time of flight mass spectrometry (MALDI-TOF MS) was done on a Bruker Reflex IV instrument (Bruker Daltonics, Billerica, MA) in the reflectron mode.

Antibody characterization

A polyclonal antiserum against synthetic fiddler crab (*Uca pugilator*) β-PDH was prepared by immunizing rabbits with a thyroglobulin/PDH conjugate exactly as described by Dircksen et al. (1987). Briefly, 1.8 mg full-length, synthetic *Uca pugilator* PDH and 6.5 mg bovine thyroglobulin (Sigma-Aldrich, Dorset, UK), in 1 ml 0.1 M phosphate buffer, pH 7.4, was conjugated with 18 μmol glutaraldehyde for 12 hours on ice and ON at 4°C, after which a further 18 μl of glutaraldehyde was added (15 minutes at room temperature). Following extensive dialysis, two New Zealand white rabbits were conventionally immunized with conjugate emulsified with Freund's adjuvant. Principles of laboratory animal care and specific national laws were followed. Specificity controls in which 1 nmol PDH was preabsorbed with 1 μl antiserum completely abolished immunostaining in sections of *Carcinus maenas* eyestalks, and dot blots of HPLC-separated *C. maenas* sinus glands showed immunoreactivity with only one fraction, previously identified as authentic PDH (Löhr et al., 1993).

Molecular cloning

cDNA synthesis and RACE

Total RNA was extracted by using TRIzol (Invitrogen, Carlsbad, CA), treated with 2 U Turbo-DNase (Ambion, Austin, TX) for 30 minutes, 37°C. Following DNase clean-up, mRNA was extracted by using Dynabeads (Dynal Oslo, Norway) and stored in 10 mM TRIS at −80°C. For 3′ rapid amplification of complementary DNA ends (RACE), mRNA extracted from 1 μg total RNA was reverse-transcribed with Superscript III (Invitrogen) at 50°C, 50 minutes by using the GeneRacer 3′oligo (dT) adapter primer. For 5′ RACE, mRNA was dephosphorylated, decapped, ligated to a 5′ RACE RNA oligo (Invitrogen), and reverse-transcribed with Superscript III by using random primers, according to the manufacturer's instructions. After reverse transcription, templates were removed by incubation with RNase H (2 U, 15 minutes, 37°C).

3′RACE was performed by using nested forward degenerate primers based on the C-terminal PDH sequence determined by Edman degradation (Table 1, Fig. 2A), and primers supplied in the GeneRacer kit. PCR reagents were as follows: 25 μl Amplitaq Gold (Applied Biosystems, Foster City, CA) 1 μl (100 μM) Epdh F1 (Table 1, Fig. 2A), 1 μl (10 μM) 3′GeneRacer primer, 1 μl 3′ RACE cDNA template in a total volume of 50 μl. PCR conditions were as follows: 94°C 9 minutes, 5 cycles of 94°C 30 seconds, 62°C 30 seconds, 72°C 30 seconds, 5 cycles of 94°C 30 seconds, 57°C 30 seconds, 72°C 30 seconds, 25 cycles of 94°C 30 seconds, 52°C 30 seconds, 72°C 30 seconds, final extension at 72°C for 7 minutes. The second (nested) PCR used the primer pairs Epdh F1n (100 μM) and the 3′ nested GeneRacer primer (10 μM), with 1 μl of the first PCR. PCR reagents were 22.5 μl Megamix Blue (Helena Biosciences, Sunderland, UK), 0.5 μl each primer. PCR conditions were 94°C 4 minutes, 35 cycles of 94°C 15 seconds, 50°C 30 seconds, 72°C 30 seconds, and final extension at 72°C for 7 minutes. 5′ RACE was performed on cDNA prepared from reverse transcription of ligated RNA as detailed above. PCR reagents were as follows: 25 μl Amplitaq gold (Applied Biosystems), 1.25 μl (10 μM) Epdh G1R (Table 1, Fig. 2A), 1.25 μl (10 μM) 5′ GeneRacer primer, 1 μl cDNA template. PCR conditions were identical to those used for 3′ RACE. The second (nested) PCR used the primer pairs Epdh G1RN (Table 1, Fig. 2A) and nested 5′ GeneRacer primer, with 0.5 μl of the first PCR reaction as template and identical PCR conditions.

To confirm sequence identity, an independent cDNA synthesis (Superscript III, with random primers) was performed. This template was used for PCR by using a high-fidelity DNA polymerase mix, DNAzyme EXT (Finnzymes Oy, Espoo, Finland) according to the manufacturer's instructions, by using gene-specific primers designed to span the open reading frame (ORF; Table 1, Fig. 2A: Epdh F GSP, Epdh R GSP). PCR conditions were as follows: 94°C 60 seconds, 35 cycles of 94°C 30 seconds, 55°C 30 seconds, 72°C 30 seconds, final extension at 72°C for 7 minutes.

TABLE 1.

Primers Used for Pigment-Dispersing Hormone (PDH) Identification, Production of cRNA Probes, and Quantitative Polymerase Chain Reaction (PCR)

Method	Primer name	Fig. 2A numbers	Sequence
PDH 3′ RACE degenerate	Epdh F1	1	GTNATGAGYGAYGCWGGWAAA
	Epdh F1N	2	ATGAGYGAYGCWGGWAAA
PDH 5′ RACE	Epdh G1 R	3	GCGACGTCGTATGAATCTCGGGTCAGTGGC
	Epdh G1RN	4	CTCGGGTCAGTGGCATCATGAGGCAGTG
Epdh gene specific	Epdh F GSP	5	ACTAGAGATATTAGTATTCGTCGCTGG
	Epdh R GSP	6	CAAGTTGATGGGGGTTAAAGAC
Epdh ISH	Epdh DIG F	7	AGAACGGTTGTGTTATTCGACTT
	Epdh DIG R	8	CAAGTTGATGGGGGTTAAAGAC
Epdh ISH T-7 adapter	Epdh DIG F-T7	9	taatacgactcactatagggagaAGAACGGTTGTGTTATTCGACTT
	Epdh DIG R-T7	10	taatacgactcactatagggagaCAAGTTGATGGGGGTTAAAGAC
Quantitative RT-PCR	Epdh taqman F	11	TGGCCCAATCACGTGACTT
	Epdh taqman R	12	CTTGGCAAGACTCGCTACGAT
	Epdh MGB probe	13	6-FAM-AGCATTTCGGAAAGAG
	Epdh STD F-T7	14	taatacgactcactatagggagaACAATGCGTTTCATCATTC
	Epdh STD R-T7	15	taatacgactcactatagggagaCAAGTTGATGGGGGTTAAAGAC
	Erpl taqman F		CTGCGGAGAAATCGCACAT
	Erpl taqman R		TTTGCTCTTTCCACGATCGA
	Erpl MGB probe		6-FAM-CGTTTCTTCCAAAAAG
	Erpl STD F-T7		taatacgactcactatagggaga
	Erpl STD R-T7		taatacgactcactatagggaga

Abbreviations: ISH, immunohistochemistry; RACE, rapid amplification of complementary DNA ends; RT, reverse transcriptase.

PCR products were electrophoresed on 2% agarose gels, and bands of expected size were excised and extracted (Perfectprep Gel Cleanup, Eppendorf, Hamburg). Specific PCR products were ligated into a PCR 4-TOPO vector and transformed (Top-10F′, Invitrogen). Plasmid DNA from positive clones containing inserts of correct sizes were purified and sequenced.

In situ hybridization

Digoxygenin (DIG)-labeled cRNA probes were made by using PCR-amplified templates containing T7-phage promoter adaptors. DNA templates for antisense probes were made by using the primer pairs Epdh DIG F and Epdh DIG R-T7, and for control (sense) probes Epdh DIG R and Epdh DIG F-T7 (Table 1, Fig. 2A). PCR conditions were as follows: 97 μl Megamix Blue, 1 μl (10 μM) each primer, 1 μl cDNA (from a randomly primed Superscript III reaction). PCR conditions were as follows: 94°C 4 minutes, 35 cycles of 94°C 30 seconds, 55°C, 72°C 30 seconds, final extension at 72°C for 7 minutes. PCR reactions were concentrated on YM30 purification cartridges (Millipore, Billerica, MA), washed several times in nuclease-free water, and finally resuspended in 20 μl of water. This template (8 μl) was used for in vitro transcription with a Megashortscript kit (Ambion), according to the manufacturer's instructions, but transcription procedures were modified to allow inclusion of DIG-UTP in the reaction. Thus the transcription conditions were as follows: 1 μl each of CTP, GTP, ATP, 0.5 μl UTP (all 75 μM), 2 μl DIG-11UTP (10 μl) (Roche Diagnostics, Mannheim, Germany), 8 μl template DNA, and water to 20 μl. Subsequent procedures for in situ hybridization were performed as previously described (Wilcockson and Webster, 2008), except that brains were treated with proteinase K (200 μg/ml, Roche Diagnostics) for 2 minutes at room temperature and then postfixed in 4% PFA in PBS for 30 minutes.

Quantitative RT-PCR

Quantitative PCR was performed by using Taqman reagents (Applied Biosystems) unless otherwise stated. Sequences and positions for primers and 5′ 6-FAM-labeled MGB hydrolysis probes are given in Table 1 and Figure 2A.

Total RNA was extracted from heads; DNAse was treated as described above and resuspended in 10 μl nuclease-free water. Then 5μl RNA from each extraction was reverse-transcribed by using Taqman high-capacity cDNA reverse transcription reagents and random primers for 120 minutes at 37°C and the reaction was terminated by heating to 85°C for 5 seconds.

Standard curves were produced by using single-species cRNA templates generated as previously described (Chung et al., 2006). A 400-bp *Epdh* DNA template containing the T7 phage promoter sites at the 3′ and 5′ ends was prepared by using Epdh standards F-T7 and Epdh standards R-T7 (Table 1, Fig. 2A) primers with 50 μl Megamix Blue PCR mix (94°C 4 minutes, 94°C 30 seconds, 55°C 30 seconds, 72°C 30 seconds for 40 cycles and a final extension of 72°C for 7 minutes). The PCR reactions

were checked for size and specificity by gel electrophoresis concentrated as described above and used in an in vitro transcription reaction (Megashortscript, Ambion). Run-off transcripts were subjected to DNAse treatment by using 2 U Turbo DNAse (Ambion) for 30 minutes at 37°C before being purified on 6 M urea-10% polyacrylamide gels. Bands of the expected size were excised and eluted from the gel with Probe Elution solution (Ambion) overnight at 37°C followed by ethanol precipitation, rapid air-drying, and resuspension in nuclease-free water (20 μl). Purified transcripts were quantified by using a Nanodrop ND-1000 (Thermo Fisher Scientific, Leicestershire, UK) absorbtion at 260 nm and converted to copy number by using Avogadro's constant/moles. Standards were diluted to 1×10^{11} copies per μl and stored at −80°C.

Quantitative PCR was performed on an Applied Biosystems 7900 thermocycler by using Taqman Universal 2x Mastermix, 0.5 μl each primer (10 μM) and probe (2.5 μM), and 1 μl template cDNA in a total volume of 25 μl per reaction. Reaction conditions were as follows: 95°C 15 seconds, 60°C 60 seconds for 40 cycles. The quantity of each transcript measured was automatically calculated by the Applied Biosystems software from the quantification threshold values (C_q values) of samples by comparing them with the C_q values obtained from the standard curves (1×10^9 to 1×10^3 copies per reaction). PCR efficiency was calculated by using the formula $E = 1 + 10^{(-1/\text{slope})}$, where slope is the gradient of the line plotted from the C_q value/log copies. For *Epdh* and the reference gene *Erpl32* (*Eurydice* ribosomal protein L32, own unpublished sequence) the PCR efficiency was >90%. *Epdh* measurements were normalized to *Erpl2* and expressed as fold change in expression relative to the 19:00 timepoint (which showed lowest *Epdh* expression).

Behavioral analysis and animal harvesting for qPCR

Eurydice were collected at high water on spring tides throughout the summer months, when the animals were most abundant, and placed immediately in 10 × 63-mm polystyrene tubes containing sand to a depth of 3 mm and 2 ml fresh seawater. In these conditions, animals could be maintained for several days without significant evaporation of seawater or reduction in oxygen levels. The tubes were returned to the laboratory and placed in *Drosophila* activity monitors (DAM-10, Trikenetics Waltham, MA) held at 15°C and constant darkness (DD). Swimming activity was recorded as infrared beam breaks on a PC by using proprietary Trikinetics software at 10-second intervals and pooled into 6-minute bins. Activity recordings were analyzed by using ClockLab software (v2.6.1) operated through MatLab v7.3.0 (The Mathworks, Natick, MA) and double-plotted with a tau of 12.4 hours. Animals showing robust circatidal swimming behavior were harvested at 4 time-points throughout the solar day at 6-hour intervals, and the heads were placed in liquid nitrogen until ready for RNA extraction. Heads taken at each time-point were pooled (about 10–20) to give sufficient RNA for accurate qPCR analysis. Samples were collected over multiple tides such that they could be combined to cover a full 24-hour period at 3-hour intervals. This sampling regime was repeated four times throughout the summer months. Activity plots taken from individual animals used for pooled qPCR experiments were combined and plotted as mean activity over time.

Chromatophore analysis

Animals were collected at night-time high tides, placed in groups of about 20 in individual light-proof containers, and removed to a temperature-controlled (ambient seawater temperature) laboratory in DD. Following a 24-hour "free run" in DD, the animals were snap-frozen in liquid nitrogen at 3-hour intervals. At the end of the sampling period, animals were individually imaged by using a digital camera attached to a dissecting microscope. Chromatophores were staged according to a modified Hogben and Slome (1931) index, which included 0.5 point scoring. To avoid possible bias, all scoring and analysis was done with the experimenter masked from the experimental treatment.

Immunohistochemistry

Cerebral and fused thoracic and abdominal ganglia were dissected under ice-chilled saline and fixed in ice-cold Stefanini's fixative (Stefanini et al., 1967) overnight at 4°C. Following fixation, tissues were washed extensively in PTX before incubation in primary antiserum diluted to 1:2,000 in PTX. Preparations were incubated overnight at 4°C before washing in PTX and application of secondary antisera. The secondary antiserum was 1:500 Alexa 488-labeled goat-anti rabbit IgG (Molecular Probes, Eugene, OR), incubated overnight at 4°C before extensive washing in PTX. Preparations were mounted in Vectashield (Vector) and visualized by using a Zeiss LSM 510 confocal microscope (Carl Zeiss Microimaging, Göttingen, Germany). Confocal images were based on a Z-stack of 10–15 optical sections taken at 1–2-μm intervals.

RESULTS

Characterization of cDNA encoding PDH

The cloning approach initially used was one involving fully degenerate forward primers in conjunction with 3′ RACE. A large number of degenerate primers based on consensus sequences of PDHs from a variety of

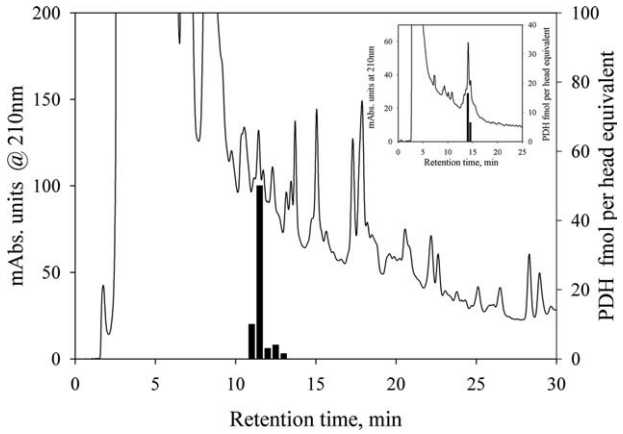

Figure 1. RP-HPLC purification of PDH from *E. pulchra*. Main chromatogram shows elution profile of an extract of 250 *Eurydice* heads. Fractions were collected automatically at 30-second intervals, and aliquots (1–2%) were assayed by EIA for PDH immunoreactivity (black bars). Immunoreactive fractions were rechromatographed to give two immunoreactive fractions (inset). Chromatographic and EIA conditions were as detailed in the text.

arthropods, and several PCR strategies were used. This approach was unsuccessful. Accordingly, we then pursued a strategy of obtaining peptide sequences by HPLC purification of head extracts and Edman microsequencing. Batchwise HPLC purification of an SPE-purified extract from 1,500 *Eurydice* heads was followed by screening via PDH EIA, and further rechromatography of immunoreactive fractions (Fig. 1). This approach yielded a single immunoreactive peak of approximately 33 pmol (*Uca pugilator* β-PDH equivalents). Microsequencing gave the following sequence: NAELINSLLGVPRVXSDA. MALDI-TOF MS of 3 pmol of material assigned a mass ($M+[H^+]$) of 1913.83 Da. The determined mass could be reconciled with the sequence if X = Met sulfoxide and C-terminal amidation. Using this information, we designed fully degenerate nested forward primers to the proposed C-terminal sequence of PDH, assuming C-terminal amidation, (VMSDAGK), and 3′ RACE reverse primers. Cloning and sequencing of the single PCR product obtained gave the information needed to construct sequence-specific primers in the 3′ UTR for 5′ RACE. This approach gave a full-length cDNA. The sequence of the ORF was reconfirmed by using a high-fidelity proofreading DNA polymerase mix.

The sequence of the cDNA is shown in Figure 2B. (GenBank accession no. GQ380440.1). The cDNA cloned and sequenced consists of a 102-bp 5′ UTR and a 204-bp 3′ UTR containing a canonical polyadenylation signal, AATAAA (Proudfoot and Brownlee, 1976). The ORF (249 bp) encodes a 24-residue signal peptide, a 38-residue precursor-related peptide, terminating in a tribasic cleavage site (RKR), and an 18-residue PDH with amidation signal (GRR). Conceptual translation of the DNA sequence for the mature peptide agreed exactly with the sequence proposed from Edman sequencing.

Expression of PDH in the brain, by in situ hybridization and immunohistochemistry

A schematic diagram showing the cerebral ganglia of *E. pulchra*, positions of PDH- expressing perikarya, and corresponding neuronal tracts is shown in Figure 3.

Whole-mount ISH of brains (and the ventral nerve cord) using DIG-labeled antisense cRNA corresponding to a 461-bp region encompassing the entire ORF (249 bp), 63 and 149 bp of the 5′ and 3′ UTR, respectively, showed that strong, unequivocal hybridization signals were restricted to two groups of cells in the protocerebrum (Fig. 4A–C). First, a prominent group of five, or occasionally six, perikarya was seen in a dorsolateral position, at the base of the optic peduncle. The larger of these cells (about 20 μm, n = 3–4) hybridized very strongly, and the cell bodies had a stellate outline (Fig. 4B), whereas the smaller cells (about 15 μm, n = 2) were rather rounded in outline and possibly hybridized less intensely. Toward the midline, and in a mid-ventral position, two 15–18-μm diameter perikarya (which invariably gave very strong hybridization signals) were observed (Fig. 4C). Although several preparations apparently indicated the presence of only one cell (i.e., Fig. 4A), because these were on the surface of the neuropil, they were frequently lost during dissection or incubation. DIG-labeled sense probes did not give any detectable signal (results not shown). The architecture of these neurons was investigated with whole-mount immunohistochemistry by using confocal microscopy (Fig. 4D,H). Two cell groups were again observed. The first, comprising five to six dorsolateral perikarya, corresponded exactly to those revealed by ISH (Fig. 4D,E,G). When antiserum (1 μl) was preabsorbed with synthetic (*Uca*) PDH, immunolabeling was completely abolished (results not shown).

The group of five to six cells projected thick, prominent axons posteriorly, which at the base of the optic peduncle, showed a characteristic T-shaped axonal morphology; a thick branch projected anteriorly, and another entered the eye peduncle (Fig. 4D,E), where they branched extensively in the laminae. Surprisingly, although the sinus gland (SG) was clearly microscopically visible, as a discrete and compact blue/white structure on the ventral margin of the eye peduncle, it could not be seen as an identifiable structure via PDH immunohistochemistry; presumably it was masked by the extensive immunopositive fibers and varicosities in the laminae of the eye peduncle (Fig. 4E). The ascending axons of the

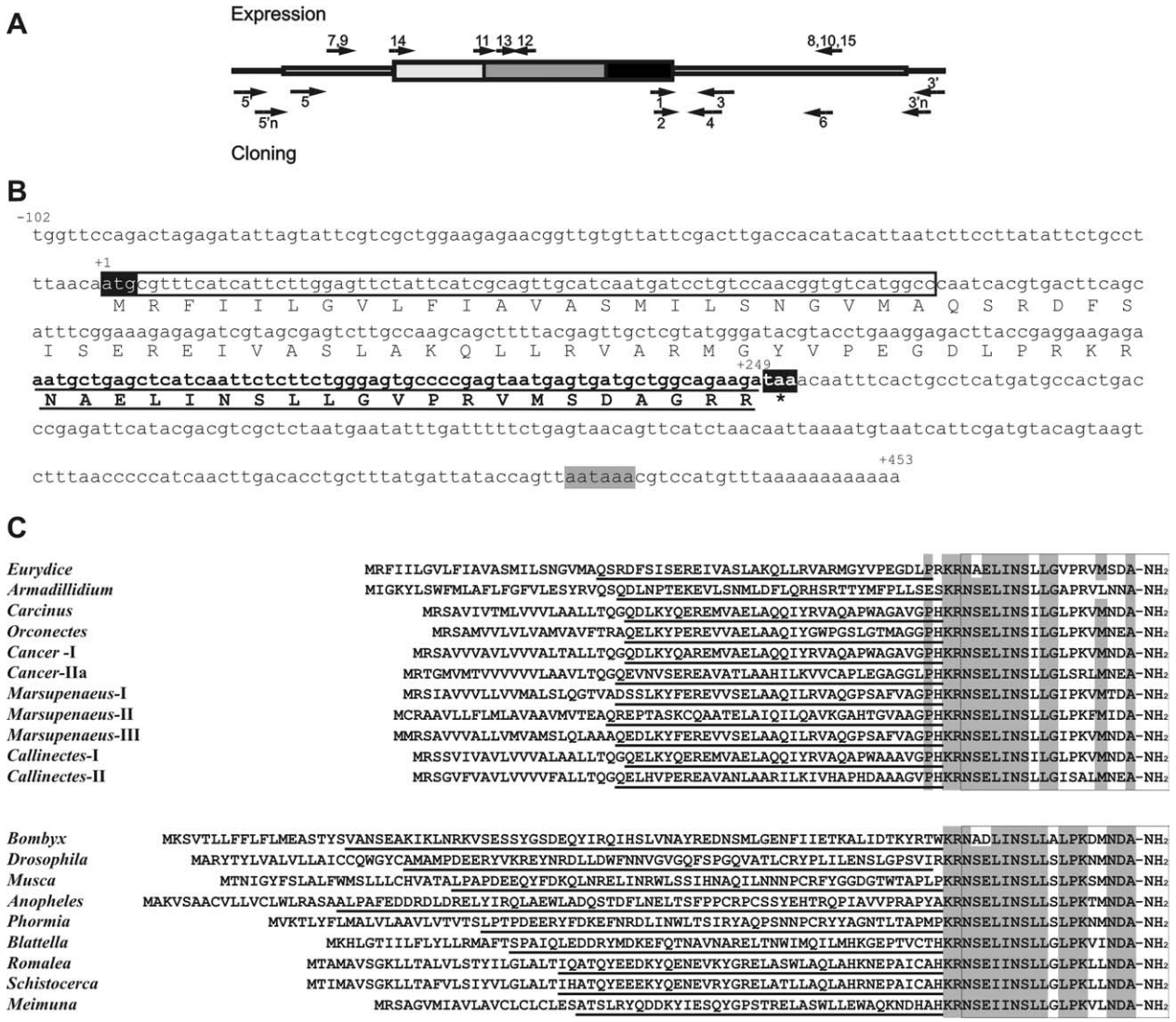

Figure 2. **A:** Schematic of full length *E. pulchra* PDH cDNA, drawn to scale, with primer positions (for gene expression and cloning) and identification numbers marked. These are detailed further in Table 1. Pale gray bar, coding region for putative signal peptide; dark gray bars, coding region for PDH precursor-related peptide; black bar, coding region for PDH. Open bars represent UTRs. Lines represent sequences added for 3′ and 5′ RACE. **B:** Nucleotide and deduced amino acid sequence for PDH from *E. pulchra*. Nucleotide numbering begins at the 5′ UTR (−102), ATG (black box) at +1, and stop codon (black box, asterisk) at +249; polyadenylation signal is shown as a gray box. Open boxed sequence indicates putative signal peptide, and underlined sequence indicates mature PDH including amidation and dibasic cleavage signal, together with conceptual translation of PDH peptide. **C:** Amino acid sequences of representative PDH/F precursor peptides from crustaceans (upper panel) and insects (lower panel). Identical residues are shaded, allowing only a single amino-acid mismatch. Putative precursor-related peptides, identified by using SignalP 3.0, are underlined. Boxes highlight mature PDH/Fs. Accession numbers are as follows: *Eurydice pulchra*, GQ380440.1: *Armadillidium vulgare*, AB543253.1; *Carcinus maenas*, L08635.1; *Orconectes limosus*, S59496.1; *Cancer productus*- I, EU009116; *Cancer productus*-IIa, EU009118; *Marsupenaeus japonicus*-I, AB073367.1; *Marsupenaeus japonicus*-II AB073368.1; *Marsupenaeus japonicus*-III, AB247562.1; *Callinectes sapidus*-I, Q23755; *Callinectes sapidus*-II Q23756; *Bombyx mori*, NP_001036920.2; *Drosophila melanogaster*, O96690.2; *Musca domestica*, AB095922.1; *Anopheles gambiae*, XM_315791.4; *Phormia regina*, AB127943.1; *Blatella germanica*, EU182248.1; *Romalea microptera*, U42472.1; *Schistocerca gregaria*, GU065715.1; *Meimuna opalifera*, AB084469.1.

T-shaped axons branched extensively, first toward the midline, where at least five axon branches could be observed (Fig. 4F). These projected ventrally, possibly both ipsi- and contralaterally, and gave rise to extensive arborizations terminating in boutons on the dorsal surface of the deuterocerebrum, in characteristic "horn-shaped" structures and in an anterior median area (Fig. 4D). The anteriorly projecting branches of these axons formed a further field of dorsal arborizations and terminal boutons on the anterior-dorsal region of the protocerebrum,

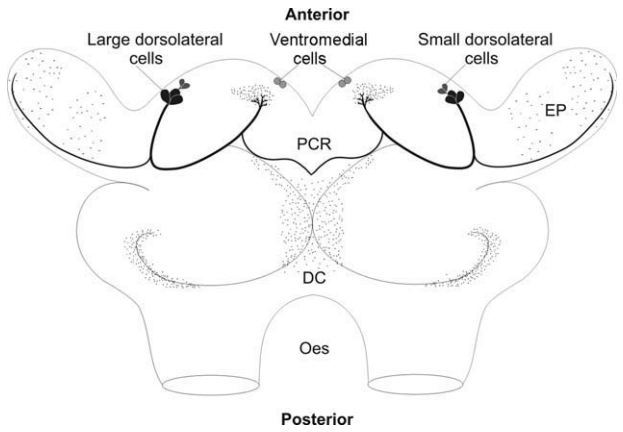

Figure 3. Schematic diagram showing a dorsal view of the cerebral and optic ganglia of *E. pulchra*. DC, deuterocerebrum; EP, eye peduncle; Oes , esophagus; PCR, protocerebrum. Stippled areas represent regions of arborizing dendrites.

directly adjacent to the two ventromedian PDH-IR neurons (Fig. 4D,E,H). Despite extensive investigations, we never observed convincing in situ hybridization signals, or immunopositive structures in the remainder of the CNS (ventral nerve cord).

Patterns of expression of Pdh mRNA during diel and tidal cycles

Freshly collected *E. pulchra* were placed under constant conditions (DD, 15°C), and sampled for a further 36 hours at 3-hour intervals to determine mean chromatophore dispersion indices. Under these conditions, animals showed dramatic, robust, and reproducible circadian rhythms of chromatophore pigment migration, such that animals displayed dispersed chromatophores (darkening) during times of expected daylight, and concentrated chromatophores (blanching) during times of expected darkness (ANOVA, $F_{1,12} = 33.1$, $P < 0.001$). Tidal components of chromatophore dispersion rhythms were never observed (Fig. 5A), although these animals showed clear tidal locomotor rhythms with a mean tau of 12.41 hours (Fig. 5B). Additionally, for animals that were not entrained (laboratory stocks held in constant darkness), rhythms of chromatophore dispersion were never observed (results not shown). To determine whether circadian changes in chromatophore dispersion might be accounted for by concomitant changes in *Epdh* gene expression, separate experiments were performed whereby *E. pulchra* heads were harvested at 3-hour intervals for 24 hours and processed for quantitative RT-PCR (Fig. 5C). No clear-cut patterns of *pdh* expression based on either tidal or circadian regimes were seen, and changes in *pdh* transcript expression over 24 hours were not significant (Kruskal-Wallis test, $P = 0.645$).

DISCUSSION

An unusual PDH in Eurydice pulchra

In order to develop tools for examining changes in *pdh* gene expression during circadian or circatidal cycles, it was mandatory to isolate full-length cDNA encoding *pdh* transcripts. Despite exhaustive attempts using degenerate PCR, based on primers designed from consensus sequences of available PDFs, this approach was unsuccessful. However, by determining the amino acid sequence empirically (by Edman microsequencing of HPLC-purified material from 1,500 *Eurydice* heads), we obtained the sequence of a molecule that was clearly PDH-like, but yet displayed some unusual features. All PDFs so far identified belong to either the α or β-PDH group (for review, see Rao, 2001), and with one exception, the N-terminus bears the sequence motif NS E/D L/ I/ INS. In *Eurydice*, S^2 is replaced by A^2, and toward the C terminus, S^{16} is unique. Although there are other amino acid substitutions found in the *Eurydice* sequence that are also found in other arthropods, it was interesting to note that in the only other isopod for which PDH sequence information is available, *Armadillidium vulgare* (Fouda et al., 2010), the common S^2 motif is present, and surprisingly, there are four other amino acids that differ in the mature peptide, and no obvious sequence similarity in their precursor-related peptides (Fig. 2C), despite taxonomic relatedness. Although a large number of PDH/Fs have been identified (representatives from both crustaceans and insects are shown in Fig. 2C), the S^2-A^2 substitution seen in *Eurydice* has, to date, only been found in the silkworm, *Bombyx mori* (Roller et al., 2008), which seems to have a rather unusual neuropeptidome compared with other insects.

Because the possibility of Edman sequencing errors remained, we determined the mass of this PDH via MALDI-TOF MS, demonstrating that it was identical to the predicted mass (with C-terminal amidation), and by cloning and sequencing full-length cDNA, using primers derived from this PDH sequence. We thus verified that the empirically determined sequence was indeed correct. With regard to the conceptual PDH precursor sequence, the PDH precursor-related peptide (PPRP; 35 residues) was rather different from currently known crustacean PDH precursors, and also was flanked by a tribasic (RKR) cleavage site rather than the dibasic (KR) site found in all other PDH/Fs except for *Drosophila* (RKR; Fig. 2C). Although the divergence of PPRP sequences between insects and crustaceans has previously been noted (Rao, 2001), the lack of relatedness of EpPDH with that of other crustacean members was striking.

With regard to the diversity of PDH-like molecules within a single species, multiple isoforms seem to be common in decapod crustaceans (Rao and Riehm, 1989;

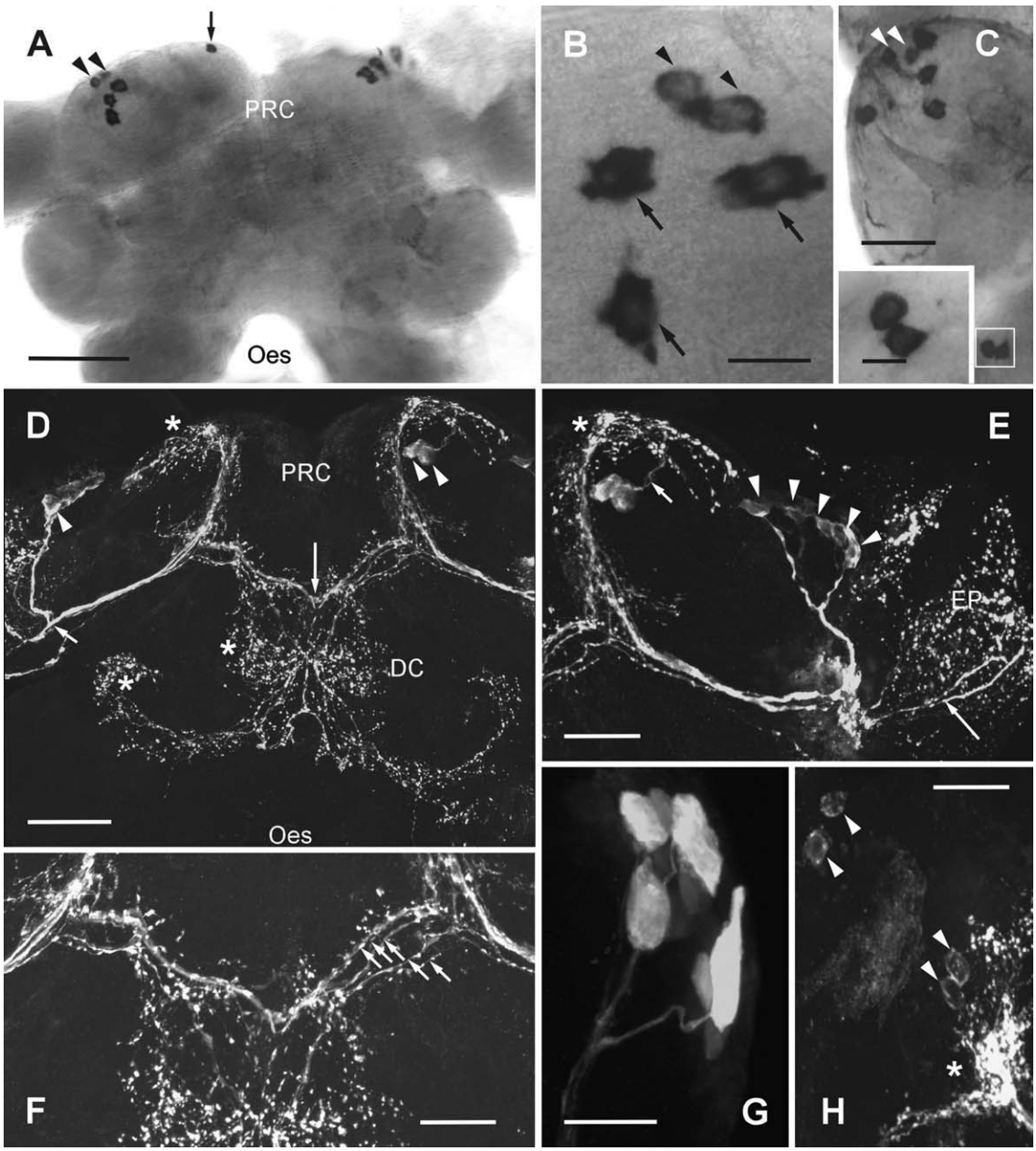

Figure 4. Expression of PDH mRNA (A–C) and peptide (D–H) in the cerebral ganglia of *E. pulchra*. **A:** Whole-mount in situ hybridization, dorsal view, of cerebral ganglia. Arrowheads indicate two perikarya in the dorsolateral cell group, slightly smaller than the main group of three to four strongly hybridizing perikarya, which exhibit a stellate outline. In this preparation a single ventromedian cell shows a strong hybridization signal (arrow). This cell is missing on the corresponding (right) protocerebrum (PRC). Oes, esophagus; DC, deuterocerebrum. **B:** Detail of dorsolateral cell group. Three of the larger (20-μm) stellate cells are visible in this preparation. Arrowheads identify smaller, less intensely hybridizing cells. **C:** In situ hybridization showing six perikarya in the dorsolateral cell group (orientation: anterior, left). Arrowheads indicate the two smaller cells shown in other preparations (A,B). Two ventromedian cells (see Fig. 3 for position in cerebral ganglia) are visible (box and inset). **D:** Whole-mount immunohistochemistry of cerebral ganglia. Arrowheads show PDH-IR somata; five to six (dorsolateral) cells. In this preparation a maximum of 5 cells were seen. These project prominent axons ventrally, which form characteristic T-shaped junctions at the base of the eye peduncle (small arrow) Ascending axons project arborizing dendrites on the surface of the median protocerebrum (asterisk), and branches projecting toward the midline (large arrow) branch extensively in the deuterocerebrum, projecting numerous arborizing dendrites on the dorsal surface (asterisks) **E:** View of the right side of the protocerebrum (the same preparation shown in D). Arrowheads show five dorsolateral cells, projecting thick, T-shaped axons. Branches of these (large arrow) enter the eye peduncle (EP). Axons from two ventromedian cells (small arrow) project into the area of arborizing dendrites (asterisks), originating from the T-shaped axons. **F:** View of branching dendrites in the midline of the posterior protocerebrum (preparation shown in D). Small arrows identify five axonal branches, projecting ipsi- and contralaterally to the extensive dorsal dendritic arborizations in the deuterocerebrum. **G:** View of the group of five dorsolateral strongly immunoreactive perikarya, projecting axons posteriorly. **H:** Two pairs of weakly immunoreactive ventromedian perikarya (arrowheads). Asterisk indicates dorsal arborizing dendrites (see D for orientation). Scale bar = 100 μm in A; 50 μm in D–H; 25 μm in F,G; 20 μm in B and inset to C.

Klein et al., 1994; Desmoucelles-Carette et al., 1996; Yang et al., 1999; Bulau et al., 2004). Notably, a recent report (Hsu et al., 2008) has convincingly demonstrated a differential distribution of β-PDH-I and -II isoforms in the eyestalk of *Cancer productus*, indicating that the former is likely to function as a neurotransmitter/modulator, whereas the latter functions as a neurohormone, and is only expressed by neurons that terminate in the SG. In contrast, in *Callinectes sapidus*, β-PDH-I was the only isoform found in the SG and was 400-fold more active than β-PDH-II in chromatophore dispersion assays (Mohrherr et al., 1990), suggesting that β-PDH-II may act as a neuromodulator/transmitter in this species. In the present study, the sequence of EpPDH appears more like the *Cancer* type I isoform, with three identical residues to type I in the nonconserved positions, but only one identical position to type II (Fig. 3B).

Because the emerging scenario for crustacean PDHs is one in which multiple isoforms are widespread, it seems possible that we have not comprehensively identified the PDH inventory in *E. pulchra*. However, only a single immunoreactive peak was observed by HPLC-EIA, and the resolution of this technique should readily separate short peptides with single amino acid differences. Furthermore, whereas the anti-PDH antibody used recognizes epitopes similar or identical in all crustacean and insect β-PDHs (Honda et al., 2006), we always observed *complete* correspondence between perikarya immunolabeled using the PDH antibody, and those hybridizing with the cRNA probe. Thus, at present, we only have firm evidence for a single species of PDH in *E. pulchra*.

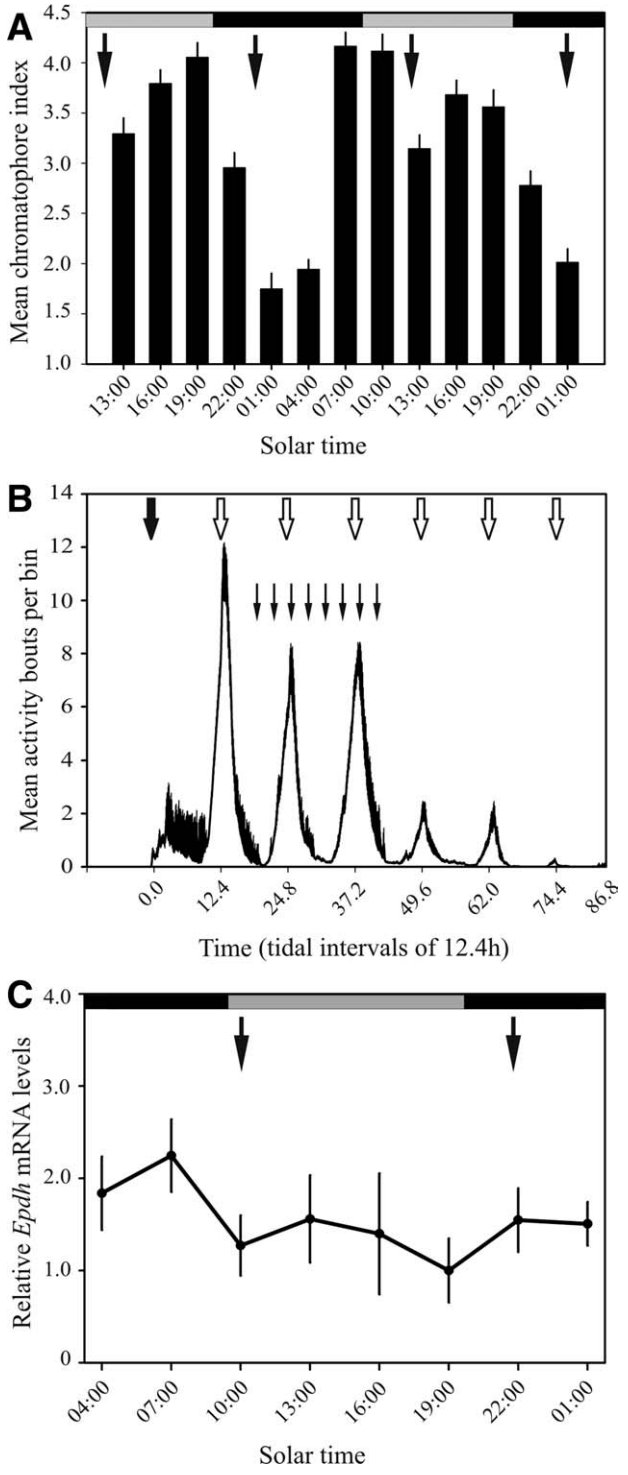

Neuroanatomy of PDH-IR neurons

The neuroanatomy of PDH-IR neurons in the eyestalk and brain of adult crustaceans (primarily decapod) crustaceans and insects has been mapped extensively (see

Figure 5. Changes in chromatophore dispersion and PDH expression in *E. pulchra* collected from the shore and held in constant (DD, 15°C) conditions. **A:** Mean chromatophore index for animals (n = 10) sampled at 3-hourly intervals for 36 hours. Shaded bar indicates times of expected light (gray)/dark (black) cycles, arrows show times of expected high water. Chromatophores showed significant changes in morphology over time (ANOVA $F_{1,12} = 33.1$, $P < 0.001$). **B:** Activity of *E. pulchra*. Animals were collected from the shore and placed in DD. Individuals showing robust tidal swimming rhythms were sacrificed for qPCR. Plots show the mean activity (± SEM) of animals recorded in *Drosophila* activity monitors. Infrared beam breaks were collected at 10-second intervals and pooled into 6-minute bins. The large solid arrows show time that animals were removed from the beach and placed in monitors. Large open arrows indicate time of expected high water on the home beach, and small black arrows point to sampling time for qPCR relative to the tidal swimming behavior. γ2 periodogram analysis revealed a mean tau of 12.4 hours (± −0.08, SEM), n = 298. **C:** Expression of *pdh* mRNA in *E. pulchra* for animals (n = 5, vertical bars = ± −1 SEM) sampled at 3-hour intervals over 24 hours. Transcript numbers were normalized against the reference gene *Erpl32*. Shaded bar and arrows are as described for A. *Epdh* abundance did not change significantly over the 24-hour sampling period ($P = 0.645$, Kruskal-Wallis test). Arrows show time of expected high water on the home beach.

Harzsch et al., 2009 for a comprehensive list). Because for insects the accessory medulla, which is an integral part of the circadian pacemaker system, contains clusters of PDF-IR somata (Homberg et al., 1991; Nässel et al., 1991, 1993; Helfrich-Förster 1995, 1997), we were interested in determining whether morphological correlates existed between the PDH-IR neurons in *Eurydice*, and those of insects, notwithstanding the apparent absence of an identified accessory medulla in the crustacean brain.

In a recent study Harzsch et al. (2009) has proposed that the large PDH-IR somata (named C, C′, C″) adjacent to the medulla interna of the eyestalk in embryonic lobster, *Homarus americanus*, correspond to those termed the large pigment-dispersing factor-like immunoreactive medulla (PDFMe) neurons by Helfrich-Förster and Homberg (1993) and Helfrich-Förster (1995, 1997). In the developing lobster embryo, these somata project thick T-shaped fibers, with very conspicuous branching points to the medulla externa, to the contralateral eyestalk, and posteriorly to the median protocerebrum. A similar arrangement of PDH-IR neurons is also seen in developing *Carcinus maenas* embryos (Chung and Webster, 2004). In *Eurydice*, five to six prominent somata, exhibiting strikingly similar morphology to those in the developing lobster and crab (i.e., thick T-shaped axons) were seen in each anterolateral protocerebrum. Although the pathways of individual axons were difficult to trace with certainty, it was clear that these somata directed axon branches to the medulla externa, where they branched extensively. Further branches projected anteriorly, arborizing extensively near two smaller PDH-IR somata in the median protocerebrum, and apparently terminating in an area of boutons on the dorsal surface of the median protocerebrum. Additionally, ipsilateral and contralateral projections were prominent, particularly those projecting posteriorly to the deuterocerebrum, where they terminated in dense fields of dorsal arborizations and boutons.

Electron microscopy studies are now vital to determine whether the boutons observed could release PDH directly into the hemolymph. However, comparison with another isopod for which detailed information of neuropetidergic anatomy is available, the woodlouse *Oniscus asellus* (Nussbaum and Dircksen, 1995), shows a broadly comparable neuronal arrangement. PDH-IR structures in the protocerebrum are represented by three ventral perikarya (PGR3) positioned between the medulla externa and medulla terminalis, with a conspicuous T-shaped axonal anatomy and two groups of cells (2, 3) in the medulla terminalis (PGR1, 2). Nevertheless, although there are arborizing dendrites near PGR1, 2 arising from the T-shaped axons of PGR3 in *Oniscus*, the most striking, and perhaps fundamental difference between *Oniscus* and *Eurydice* PDH neuroanatomy is that the very conspicuous field of arborizing dendrites on the dorsal surface of the deuterocerebrum seen in *Eurydice* is entirely lacking in *Oniscus*. In a recent description of PDH-IR neurons in another terrestrial isopod, *Armadillidium vulgare* (Fouda et al., 2010), the distribution of PDH neurons (visualized by IHC and ISH) was rather different from those described for *Eurydice* and *Oniscus*. Apart from some neurons in the anterior protocerebrum that could be homologous to the PGR neurons, numerous others were seen in the accessory lobe and tritocerebrum (subesophageal ganglion). The axon tracts and arborizing dendrites that were so conspicuous in the deuterocerebrum of *Eurydice* were notably absent in *Armadillidium*.

A comparison of the results obtained here with those of Harzsch et al. (2009) indicates that it is very likely that the PDH-IR neurons exhibiting T-shaped axonal morphology in *Eurydice* are equivalent to the PDFMe neurons near the accessory medulla of insects. Because this is an integral part of the circadian pacemaker system in insects, it is tempting to suggest that this may also be the case in Crustacea. With regard to the small PDH-IR neurons observed near the midline of the brain, these would seem to correspond to those in the X-organ of other crustaceans and are adjacent to two median pairs of large crustacean hyperglycemic hormone (CHH) immunoreactive neurons (unpublished observations). In the lobster, equivalent neurons have been identified (Harzsch et al., 2009) as homologous to the PDF-like immunoreactive calyx neurons in *Drosophila* (Helfrich-Förster, 1995, 1997) or posterior dorsal neurons in *Phormia* (Nässel et al., 1993).

Circadian color change rhythms and expression of Pdh mRNA

It has long been known that many malacostracan crustaceans exhibit circadian (and occasionally, circatidal) color change phenomena, involving endogenous rhythms of pigment dispersion and concentration in their chromatophores and distal eye pigment cells (Brown et al., 1953; Fingerman, 1955). The molecular basis of the clockwork controlling such rhythms has, to our knowledge, not been studied in crustaceans. Because PDF is a key transmitter in the rhythmic control of circadian phenomena in insects, and particularly in view of the fact that any chromatophore dispersion rhythms in crustaceans must reflect concomitant patterns of release of PDH into the hemolymph, we determined the endogenous rhythms of chromatophore dispersion in *Eurydice* and attempted to correlate this phenotype with transcriptional changes in *pdh* mRNA. Because neurohormone release following depolarization is often (but not always) associated with changes in mRNA transcription rates (for review, see

MacArthur and Eiden, 1996), an interesting hypothesis would be that color change rhythms and *pdh* mRNA transcription might be coupled. Furthermore, because *Eurydice* exhibits strong endogenous circatidal swimming activity (Hastings, 1981a,b), we were interested to see whether this might also be reflected in changes in *pdh* transcription.

Robust endogenous circadian color change rhythms, in which chromatophores were maximally dispersed during subjective day and concentrated during subjective night were observed, as well as a strong endogenous circatidal locomotor rhythm. Nevertheless, there appeared to be no obvious circadian or circatidal rhythm in *pdh* transcript abundance. In *Drosophila*, cycling of *pdf* transcript levels is modest at best (Park and Hall, 1998), and it seems that the only circadian phenotype involves immunoreactivity in axon terminals of the small lateroventral neurons (s-LN_vs) (Park et al., 2000; Nitabach et al., 2006). Because the robust circadian chromatophore rhythm can *only* reflect changes in secretion of PDH, it would be interesting to examine corresponding changes in PDH accumulation at neurosecretory terminals in *Eurydice*. Classically, in view of its role as the sole neurosecretory tissue in the eye of malacostracan crustaceans, the sinus gland would appear to be the relevant tissue of interest in this context. However, although the sinus gland is easily microscopically visible in *Eurydice*, it was difficult to visualize against the complex background of arborizing dendrites in the eye, even with confocal microscopy. The sparsely distributed PDH-immunopositive axon terminals in the sinus gland of *Oniscus* has been commented upon (Nussbaum and Dircksen, 1995), and there seems to be few immunoreactive terminals in the sinus gland of *Armadillidium* (Fouda et al., 2010).

Thus, it might be tempting to suggest that release of PDH from other, diffuse neurohemal areas might be more important with respect to color change rhythms. Although there are extensive dendritic fields on the dorsal surface of the brain, (clearly innervated by PDH-containing neurons that possess morphologies similar to the l-LN_vs and s-LN_vs clock neurons in the insect medulla), which appear to have morphologies strongly suggestive of a diffuse neurohemal tissue, this clearly needs critical examination at an ultrastructural level, before speculating further. It would be interesting to determine whether circadian changes in (say) secretory granule density in PDH-containing terminals or fluorescence of immunolabeled whole-mounted brains could be correlated with chromatophore dispersion. Circadian remodeling in the axon terminals of the PDF circuit has been observed in *D. melanogaster* (Fernandez et al., 2008), and changes in the morphology of PDF-containing neurites (varicosities and dense-core vesicles) have been reported in *Musca domestica* (Pyza and Meinertzhagen, 1997; Miśkiewicz et al., 2008).

Of particular interest is the recent finding that PDH-IR neurons (Cluster 6) in the brain photoreceptor neuropil of the protocerebrum of the crayfish, *Cherax destructor*, show circadian changes in expression of PDH, measured as changes in relative fluorescence intensity in fluorescently immunolabeled preparations (Sullivan et al., 2009). Thus, further investigation of the *Eurydice* PDH network and its influence on circadian (and possibly tidal) phenotypes is now timely and will significantly illuminate the neurobiology of biological oscillations in Crustacea.

LITERATURE CITED

Abramowitz A. 1937. The chromatophorotropic hormones of the crustacean: standardization, properties and physiology of the eyestalk glands. Biol Bull 72:344–365.

Aréchiga H, Rodríguez-Sosa L. 1998. Circadian clock function in isolated eyestalk tissue of crayfish. Proc R Soc Lond (Biol) 265:1819–1823.

Brown FA, Fingerman M, Sandeen MI, Webb HM. 1953. Persistent diurnal and tidal rhythms of colour change in the fiddler crab *Uca pugnax*. J Exp Zool 123:29–60.

Bulau P, Meisen I, Schmitz T, Keller R, Peter-Katalinić J. 2004. Identification of neuropeptides from the sinus gland of the crayfish *Orconectes limosus* using nanoscale on-line liquid chromatography tandem mass spectrometry. Mol Cell Proteomics 3:558–564.

Chung JS, Webster SG. 2004. Expression and release patterns of neuropeptides during embryonic development and hatching in the green shore crab, *Carcinus maenas*. Development 131:4751–4761.

Chung JS, Wilcockson DC, Zmora N, Zohar Y, Dircksen H, Webster SG. 2006. Identification and developmental expression of mRNAs encoding crustacean cardioactive peptide (CCAP) in decapod crustaceans. J Exp Biol 209: 3862–3872.

Desmoucelles-Carette C, Sellos D, Van Wormhoudt A. 1996. Molecular cloning of the precursors of pigment dispersing hormone in crustaceans. Biochem Biophys Res Commun 221:739–743.

Dircksen H, Zahnow CA, Gaus G, Keller R, Rao KR, Riehm JP. 1987. The ultrastructure of nerve endings containing pigment-dispersing hormone (PDH) in crustacean sinus glands: identification by an antiserum against a synthetic PDH. Cell Tissue Res 250:377–387.

Fanjul-Moles ML, Prieta-Sagredo A. 2003. The circadian system of crayfish: a developmental approach. Microsc Res Tech 60:291–301.

Fernández MP, Berni J, Ceriani MF. 2008. Circadian remodelling of neuronal circuits involved in rhythmic behaviour. PLoS Biol 6:e69.

Fingerman M. 1955. Persistent daily and tidal rhythms of colour change in *Callinectes sapidus*. Biol Bull 109:255–264.

Fouda M, Hiragaki S, Tufail M, Shao Q-M, Takeda M. 2010. Precursor structure, distribution and possible functions of pigment-dispersing hormone (PDH) in the terrestrial isopod *Armadillidium vulgare* (Latreille). J Insect Physiol 56: 1728-1737.

Harzsch S, Dircksen H, Beltz BS. 2009. Development of pigment-dispersing hormone-immunoreactive neurons in the American lobster: homology to the insect circadian pacemaker system? Cell Tissue Res 335:417–429.

Hastings MH. 1981a. The entraining effect of turbulence on the circatidal activity rhythm and its semilunar modulation in *Eurydice pulchra*. J Mar Biol Assoc UK 61:151–160.

Hastings MH. 1981b Semilunar variations of endogenous circatidal rhythms of activity and respiration in the isopod *Eurydice pulchra*. Mar Ecol Prog Ser 4:85–90.

Helfrich-Förster C. 1995. The *period* clock gene is expressed in central nervous system neurons which also produce a neuropeptide that reveals the projections of circadian pacemaker cells within the brain of *Drosophila melanogaster*. Proc Natl Acad Sci U S A 92:612–616.

Helfrich-Förster C. 1997. Development of pigment-dispersing hormone-immunoreactive neurons in the nervous system of *Drosophila melanogaster*. J Comp Neurol 380:335–354.

Helfrich-Förster C, Homberg U. 1993. Pigment-dispersing hormone-immunoreactive neurons in the nervous system of wild-type *Drosophila melanogaster* and of several mutants with altered circadian rhythmicity. J Comp Neurol 337: 177–190.

Helfrich-Förster C, Täuber M, Park JH, Mühlig-Versen M, Schneuwly S, Hofbauer A. 2000. Ectopic expression of the neuropeptide pigment-dispersing factor alters behavioral rhythms in *Drosophila melanogaster*. J Neurosci 20: 3339–3353.

Hogben LT, Slome D. 1931. The pigmentary effector system. VI. The dual character of endocrine coordination in amphibian colour change. Proc R Soc Lond B 108:10–53.

Homberg U. 1994. Distribution of neurotransmitters in the insect brain. In: Progress in zoology, vol 40. New York: Fischer.

Homberg U, Würden S, Dircksen H, Rao KR. 1991. Comparative anatomy of pigment-dispersing hormone-immunoreactive neurons in the brain of orthopteroid insects. Cell Tissue Res 266:343–357.

Honda T, Matsushima A, Sumida K, Chuman Y, Sakaguchi K, Onoue H, Meinertzhagen IA, Shimohigashi Y, Shimohigashi M. 2006. Structural isoforms of the circadian neuropeptide PDF expressed in optic lobes of the cricket *Gryllus bimaculatus*: immunochemical evidence from specific monoclonal antibodies. J Comp Neurol 499:404–421.

Hsu YW, Stemmler EA, Messinger DI, Dickinson PS, Christie AE, de la Iglesia HO. 2008. Cloning and differential expression of two beta-pigment-dispersing hormone (β-PDH) isoforms in the crab *Cancer productus*: evidence for authentic beta-PDH as a local neurotransmitter and beta PDH II as a humoral factor. J Comp Neurol 508:197–211.

Klein JM, Mohrherr CJ, Sleutels F, Riehm JP, Rao KR. 1994. Molecular cloning of two pigment-dispersing hormone (PDH) precursors in the blue crab *Callinectes sapidus* reveals a novel member of the PDH neuropeptide family. Biochem Biophys Res Commun 205:410–416.

Lee CM, Su MT, Lee HJ. 2009. Pigment dispersing factor: an output regulator of the circadian clock in the German cockroach. J Biol Rhythms 24:35–43.

Löhr J, Klein J, Webster SG, Dircksen H. 1993. Quantification, immunoaffinity purification and sequence analysis of a pigment dispersing hormone of the shore crab *Carcinus maenas*. Comp Biochem Physiol B 104:699–706.

MacArthur L, Eiden, L. 1996. Neuropeptide genes: targets of activity-dependent signal transduction. Peptides 17: 721–728.

Mangerich S, Keller R. 1988. Localization of pigment-dispersing hormone (PDH) immunoreactivity in the central nervous system of *Carcinus maenas* and *Orconectes limosus* (Crustacea) with reference to FMRF-amide immunoreactivity in *O. limosus*. Cell Tissue Res 253:199–208.

Mangerich S, Keller R, Dircksen H, Rao KR, Riehm JP. 1987. Immunocytochemical localization of pigment-dispersing hormone (PDH) and its coexistence with FMRFamide-immunoreactive material in the eyestalks of the decapod crustaceans *Carcinus maenas* and *Orconectes limosus*. Cell Tissue Res 250:365–375.

Miśkiewicz K, Schürmann FW, Pyza E. 2008. Circadian release of pigment-dispersing factor in the visual system of the housefly, *Musca domestica*. J Comp Neurol 509:422–435.

Mohrherr CJ, Rao KR, Riehm JP, Morgan WT. 1990. Isolation of b-PDH from sinus glands of the blue crab, *Callinectes sapidus*. Am Zool 30:28A.

Nässel DR, Shiga S, Wikstrand EM, Rao KR. 1991. Pigment dispersing hormone immunoreactive neurons and their relation to serotonergic neurons in the blowfly and cockroach visual system. Cell Tissue Res 266:511–523.

Nässel DR, Shiga S, Mohrherr CJ, Rao KR. 1993. Pigment-dispersing hormone-like peptide in the nervous system of the flies *Phormia* and *Drosophila*: immunocytochemistry and partial characterization. J Comp Neurol 331:183–198.

Naylor E. 1996. Crab clockwork: the case for interactive circatidal and circadian oscillators controlling rhythmic locomotor activity of *Carcinus maenas*. Chronobiol Int 13: 153–161.

Naylor E. 2010. Chronobiology of marine organisms. Cambridge: Cambridge University Press.

Nitabach MN, Wu Y, Sheeba V, Lemon WC, Strumbos J, Zelensky PK, White BH, Holmes TC. 2006. Electrical hyperexcitation of lateral ventral pacemaker neurons desynchronizes downstream circadian oscillators in the fly circadian circuit and induces multiple behavioural periods. J Neurosci 26: 479–489.

Nussbaum T, Dircksen H. 1995 neuronal pathways of classical crustacean neurohormones in the central nervous system of the woodlouse, *Oniscus asellus* (L.). Philos Trans R Soc Lond B 347:139–154.

Palmer JD. 2001. The clocks controlling the tide-associated rhythms of intertidal animals. BioEssays 22:32–37.

Park JH, Hall JC. 1998. Isolation and chronobiological analysis of a neuropeptide pigment-dispersing factor gene in *Drosophila melanogaster*. J Biol Rhythms 13:219–228.

Park JH, Helfrich-Förster C, Lee G, Liu L, Rosbash M, Hall JC. 2000. Differential regulation of circadan pacemaker output by separate clock genes in *Drosophila*. Proc Natl Acad Sci U S A 97:3608–3613.

Petri B, Stengl M. 1997. Pigment-dispersing hormone shifts the phase of the circadian pacemaker of the cockroach *Leucophaea maderae*. J Neurosci 17:4087–4093.

Powell BL. 1962 Types, distribution and rhythmical behaviour of the chromatophores of juvenile *Carcinus maenas* (L.). J Anim Ecol 31:251–261.

Proudfoot NJ, Brownlee GG. 1976. 3′-Non-coding region sequences in eukaryotic messenger RNA. Nature 263: 211–214.

Pyza E. 2002. Dynamic structural changes of synaptic contacts in the visual system of insects. Microsc Res Tech 58: 335–344.

Pyza E, Meinertzhagen IA. 1996. Neurotransmitters regulate rhythmic size changes amongst cells in the fly's optic lobe. J Comp Physiol (A) 178:33–45.

Pyza E, Meinertzhagen IA. 1997. Neurites of period-expressing PDH cells in the fly's optic lobe exhibit circadian oscillations in morphology. Eur J Neurosci 9:1784–1788.

Pyza E, Meinertzhagen IA. 1998. Neurotransmitters alter the numbers of synapses and organelles in photoreceptor terminals in the lamina of the housefly, *Musca domestica*. J Comp Physiol (A) 183:719–727.

Rao KR. 2001. Crustacean pigmentary-effector hormones: chemistry and functions of RPCH, PDH, and related peptides. Am Zool 41:364–379.

Rao KR, Riehm JP. 1989. The pigment-dispersing hormone family: chemistry, structure-activity relations, and distribution. Biol Bull 177:225–229.

Rao KR, Riehm JP. 1993. Pigment-dispersing hormones. Ann N Y Acad Sci 680:78–88.

Renn SCP, Park JH, Rosbash M, Hall JC, Taghert PH. 1999. A *pdf* neuropeptide gene mutation and ablation of PDF neurons each cause severe abnormalities of behavioural circadian rhythms in *Drosophila*. Cell 99:791–802.

Roller L, Yamanaka N, Watanabe K, Daubnerová I, Žitňan D, Kataoka H, Tanaka Y. 2008. The unique evolution of neuropeptide genes in the silkworm *Bombyx mori*. Insect Biochem Mol Biol 38:1147–1157.

Sehadová H, Sauman I, Sehnal F. 2003. Immunocytochemical distribution of pigment dispersing hormone in the cephalic ganglia of polyneopteran insects. Cell Tissue Res 312: 113–125.

Sousa GL, Lenz PH, Hartline DK, Christie AE. 2008. Distribution of pigment dispersing hormone- and tachykinin-related peptides in the central nervous system of the copepod crustacean *Calanus finmarchicus*. Gen Comp Endocrinol 156:454–459.

Stefanini M, Demartino C, Zamboni L. 1967. Fixation of ejaculated spermatozoa for electron microscopy. Nature 216: 173–174.

Strausfeld NJ. 2005. The evolution of crustacean and insect opic lobes and origin of chiasmata. Arthropod Struct Dev 34:235–256.

Strauss J, Dircksen H. 2010. Circadian clocks in crustaceans: identified neuronal and cellular systems. Front Biosci 15: 1040–1074.

Sullivan JM, Genco MC, Marlow ED, Benton JL, Beltz BS, Sandeman DC. 2009. Brain photoreceptor pathways contributing to circadian rhythmicity in crayfish. Chronobiol Int 26: 1136–1168.

Verde MA, Barriga-Montoya C, Fuentes-Pardo B. 2007. Pigment dispersing hormone generates a circadian response to light in the crayfish, *Procambarus clarkii*. Comp Biochem Physiol A 147:983–992.

Webster SG. 1998. Peptidergic neurons in barnacles: an immunohistochemical study using antisera raised against crustacean neuropeptides. Biol Bull 195:282–289.

Wilcockson DC, Webster SG. 2008. Identification and developmental expression of mRNAs encoding putative insect cuticle hardening hormone, bursicon in the green shore crab *Carcinus maenas*. Gen Comp Endocrinol 156:113–125.

Yang W-J, Aida K, Nagasawa H. 1999. Characterization of chromatophorotropic neuropeptides from the Kuruma prawn *Penaeus japonicus*. Gen Comp Endocrinol 114: 415–424.